

## Decomposition of NO by Microwave Discharge of NO/He or NO/Ar Mixtures

Masaharu Tsuji,\* Kousuke Nakano,<sup>†</sup> Jun Kumagae,<sup>†</sup> and Takeshi Tsuji

Institute of Advanced Material Study, Kyushu University, Kasuga, Fukuoka 816-8580

<sup>†</sup>Department of Applied Science for Electronics and Materials, Graduate School of Engineering Sciences, Kyushu University, Kasuga, Fukuoka 816-8580

(Received September 14, 2001)

The decomposition of NO into N<sub>2</sub> and O<sub>2</sub> by a continuous or pulsed microwave discharge of NO/He or NO/Ar mixtures was studied at NO and rare-gas flow rates of 2–50 and 1000 sccm, respectively. Although discharge could be maintained in the low total-pressure range of 1–350 Torr for an NO/He mixture, stable microwave discharge could be maintained in the wide total-pressure range of 1–760 Torr for an NO/Ar mixture at a microwave power of 200 W. The decomposition efficiency of NO was measured as a function of the microwave power and of the NO flow rate in a continuous mode, and as a function of the duty cycle and the pulse period in a pulse mode. The decomposition mechanism of NO in He and Ar discharges is discussed on the basis of mass spectroscopic and emission spectroscopic data.

Since NO<sub>x</sub> are major sources of acid rain, photochemical smog formation, and the greenhouse effect, new low-cost removal technologies are being developed to overcome current NH<sub>3</sub>-SCR (selective catalytic reduction) processes. Various direct decomposition methods into N<sub>2</sub> and O<sub>2</sub> in an electric discharge and plasma-assisted catalytic systems have been proposed as new promising removal techniques of NO<sub>x</sub>.<sup>1–13</sup> If NO<sub>x</sub> can be converted into N<sub>2</sub> and O<sub>2</sub> without using a catalyst or reductants such as NH<sub>3</sub> and oils, a clean convenient removal process can be developed.

Recently much attention has been given to efficient decomposition of NO using a microwave discharge and microwave discharge-assisted catalytic systems.<sup>2–9</sup> An advantage of the microwave discharge compared with a pulsed streamer corona discharge widely used for NO<sub>x</sub> removal<sup>10–13</sup> is the lack of electrodes, which are generally damaged during discharge. We have recently applied a microwave discharge to the removal of NO.<sup>2</sup> Although NO must be removed in the presence of N<sub>2</sub> and O<sub>2</sub> at atmospheric pressure for practical applications, the removal of NO diluted in He was studied at a low total pressure of about 1.0 Torr (1 Torr = 133.33 Pa) as the first step of our investigation.<sup>2</sup> The conversion of NO diluted in He was measured as a function of the microwave power at constant NO flow rates of 25, 50, and 100 sccm (standard cubic centimeter per minute) in order to examine the optimum decomposition conditions. The decomposition efficiency and discharge products of NO were analyzed using mass spectrometry and optical emission spectroscopy. We found that about 97% of NO could be decomposed into N<sub>2</sub> and O<sub>2</sub> at a low NO flow rate of 25 sccm by a microwave discharge of NO/He mixtures in the microwave-power range of 150–200 W without the need of any additives.

As the second step of our investigation, the decomposition of NO by a microwave discharge of NO diluted in Ar as well as

He was studied here at higher total pressures. The decomposition efficiency and discharge products of NO are analyzed using mass spectrometry. The decomposition mechanism of NO in He and Ar discharges is discussed on the basis of mass spectrometric and optical emission spectroscopic data.

### Experimental

The discharge-flow apparatus used for the study of NO removal is shown in Fig. 1. It consisted of a quartz discharge tube, a stainless-steel main flow tube, and an ULVAC MSQ400 quadrupole mass spectrometer (QMS). The discharge-flow apparatus was

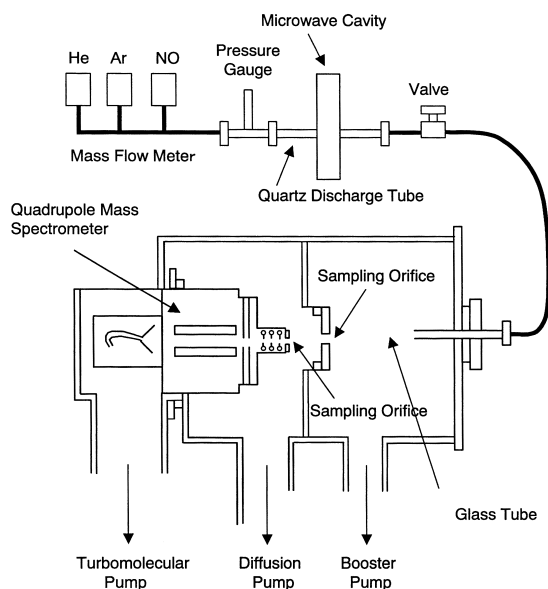


Fig. 1. Discharge-flow apparatus for the decomposition of NO.

continuously evacuated using a  $5 \text{ m}^3 \text{ min}^{-1}$  booster pump at the low-pressure range of 1–100 Torr and a  $0.06 \text{ m}^3 \text{ min}^{-1}$  rotary oil pump at the high-pressure range of 100–760 Torr. The flow rate of He or Ar was kept at 1000 sccm, while that of NO was varied in the 2–50 sccm range. Various mixtures of He or Ar and NO were fed into a microwave discharge (Koike Engineering MR-301) operated at an output power of 50–200 W. The total pressure was varied by closing a variable gate valve placed between the decomposition cell and the main flow tube. The pressure in the reaction cell was monitored using a capacitance manometer. The total pressure was varied from 50 to 400 Torr for NO/He mixtures and from 50 to 760 Torr for NO/Ar mixtures. The mass spectra of discharge products were measured using a stainless-steel sampling orifice attached to the end of the main flow tube and another stainless-steel sampling orifice attached to the front of the QMS. The internal diameters of the former and latter orifices were 3 and 0.1–1.8 mm, respectively. The relative sensitivity of QMS for NO,  $\text{N}_2$ , and  $\text{O}_2$  was calibrated using their standard gases.

## Results and Discussion

### Decomposition of NO/He and NO/Ar Mixtures by Microwave Discharge at Various Total Pressures.

When mass spectra of NO/He mixtures were measured by switching off the microwave discharge, a strong  $\text{He}^+$  peak and weak  $\text{NO}^+$ ,  $\text{N}_2^+$ ,  $\text{N}^+$ , and  $\text{O}^+$  peaks were observed due to electron-impact ionization of He, NO, and background  $\text{N}_2$ , as shown in Fig. 2(a). In addition, a weak  $\text{CO}_2^+$  and/or  $\text{N}_2\text{O}^+$  peak is observed at  $m/z = 44$ . When the discharge was switched on, the  $\text{NO}^+$  peak became weak, while the  $\text{N}_2^+$  peak became strong and an  $\text{O}_2^+$  peak appeared, as shown in Fig. 2(b). The intensi-

ty of the  $\text{CO}_2^+$  and/or  $\text{N}_2\text{O}^+$  peak at  $m/z = 44$  was essentially unchanged, when the discharge was switched on. In our recent study of  $\text{N}_2\text{O}$  removal,<sup>14,15</sup> we found that the  $\text{N}_2\text{O}^+$  peak became very weak by the decomposition of  $\text{N}_2\text{O}$  in a microwave discharge of  $\text{N}_2\text{O}/\text{He}$  mixtures. This indicates that  $\text{N}_2\text{O}$  is efficiently decomposed by a microwave discharge of  $\text{N}_2\text{O}/\text{He}$  mixtures. Thus, the  $m/z = 44$  peak observed in this study was attributed to  $\text{CO}_2^+$  arising from background  $\text{CO}_2$  in the QMS chamber. The  $\text{NO}_2^+$  peak was not observed under any conditions in our experiments. The observation of  $\text{N}_2^+$  and  $\text{O}_2^+$  peaks in the mass spectrum of discharge products implies that the corresponding neutral  $\text{N}_2$  and  $\text{O}_2$  molecules are produced by the microwave discharge of NO/He mixtures. The decomposition efficiency of NO was determined by the reduction of the intensity of  $\text{NO}^+$  peak. The formation ratios of  $\text{N}_2$  and  $\text{O}_2$  are defined as the  $[\text{N}_2]/[\text{NO}]_0$  and  $[\text{O}_2]/[\text{NO}]_0$  ratios, where  $[\text{NO}]_0$  is an initial concentration of NO before decomposition. They were estimated from the relative intensities of product  $\text{N}_2^+$  and  $\text{O}_2^+$  peaks to that of the  $\text{NO}^+$  peak before decomposition. When He was replaced by Ar, similar mass spectra were observed except for the appearance of a strong  $\text{Ar}^+$  peak and the lack of the  $\text{He}^+$  peak. On the basis of mass spectroscopic data, we conclude that NO diluted in He or Ar was decomposed exclusively into  $\text{N}_2$  and  $\text{O}_2$  as



and that the formation of  $\text{NO}_2$  and  $\text{N}_2\text{O}$  was negligible within our discharge conditions. In all the experiments reported here, the relations  $[\text{N}_2] \approx [\text{O}_2]$  and  $([\text{N}_2] + [\text{O}_2] + [\text{NO}])/[\text{NO}]_0 \approx 1.0$  were observed, indicating that the mass balance was held before and after decomposition.

In order to examine the effects of the total pressure, the decomposition efficiency of NO was measured as a function of the total pressure at a constant microwave power and flow rates of a rare gas and NO. Figures 3(a) and 3(b) show the conversion of NO and the formation ratios of products in NO/He and NO/Ar mixtures as a function of the total pressure at a microwave power of 200 W. Although it was difficult to maintain discharge above 350 Torr in an NO/He mixture under these operating conditions, stable discharge could be maintained even under atmospheric pressure in an NO/Ar mixture. The conversion of NO in the NO/He mixture was  $\geq 93\%$  in the total-pressure range of 50–350 Torr. On the other hand, the conversion of NO in the NO/Ar mixture decreases from 96 to 62% with increasing total pressure from 50 to about 500 Torr and increases from 62 to 70% in the total-pressure range of 500–760 Torr. On the basis of the experimental data shown in Figs. 3(a) and 3(b), the decomposition efficiency of NO in the NO/He mixture is higher than that in the NO/Ar mixture in the same total-pressure range of 50–350 Torr, though the discharge could not be maintained at  $> 350$  Torr in the NO/He mixture. The energies required for the decomposition of NO were calculated to be  $1.7 \times 10^4$  kJ/mol in the NO/Ar mixture at 760 Torr and  $1.3 \times 10^4$  kJ/mol in the NO/He mixture at 350 Torr.

**Decomposition of NO/He and NO/Ar Mixtures by Microwave Discharge at High Total Pressure.** In order to obtain further information on the decomposition of NO at high

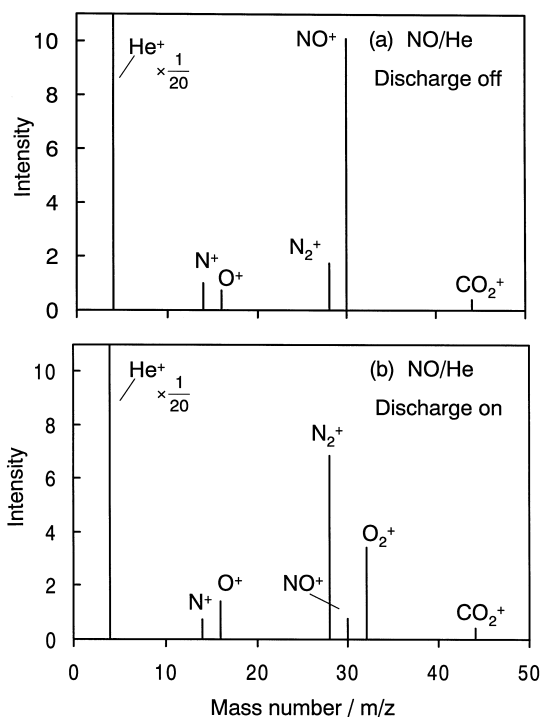


Fig. 2. Typical mass spectra of NO in an NO/He mixture obtained by switching the microwave discharge (a) off and (b) on at an NO flow rate of 100 sccm and a microwave power of 200 W. The initial concentration of NO was 90900 ppm.

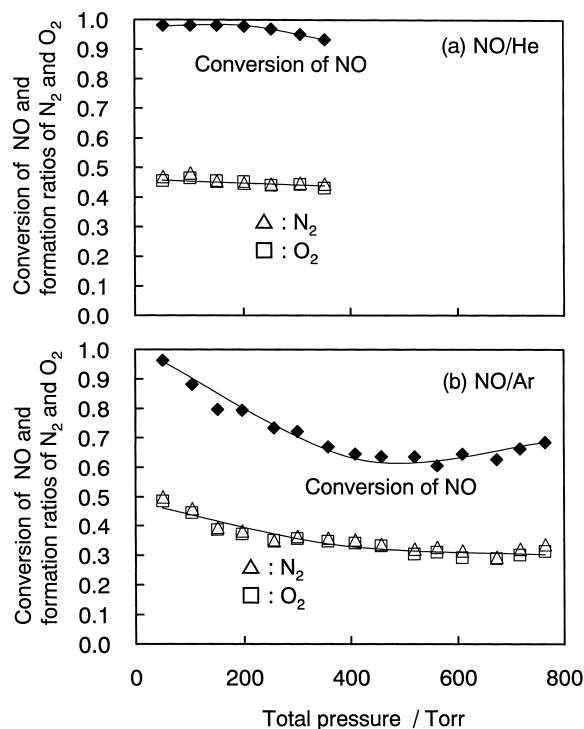


Fig. 3. Dependence of conversion of NO and formation ratios of  $N_2$  and  $O_2$  on the total pressure at an NO flow rate of 25 sccm and a microwave power of 200 W in (a) NO/He and (b) NO/Ar mixtures. The initial concentration of NO was 24400 ppm.

pressures, we measured the dependence of the decomposition efficiency and discharge products on the NO flow rate and the microwave power. Figures 4(a) and 4(b) show the dependence of the conversion of NO and the formation ratios of products on the NO flow rate in an NO/He mixture at 100 Torr and in an NO/Ar mixture at 760 Torr at a microwave power of 200 W, respectively. The conversion of NO in the NO/He mixture slightly decreases from 100 to 97% with an increase in the NO flow rate from 2 to 50 sccm. On the other hand, the conversion of NO in the NO/Ar mixture decreases from 91 to 63% with an increase in NO flow rate from 2 to about 25 sccm, and slightly increases from 63 to 70% in the high NO flow-rate range of 25–50 sccm.

Figures 5(a) and 5(b) show the dependence of the conversion of NO and the formation ratios of products on the microwave power. The conversion of NO in the NO/He mixture at 100 Torr increases from 78 to 98% with increasing microwave power from 50 to 100 W and it remained at 98% in the power range of 100–200 W. On the other hand, the conversion of NO in the NO/Ar mixture at 760 Torr increases from 20 to 62% with increasing microwave power from 50 to 200 W.

All of the above results were obtained using a microwave discharge operated in a continuous mode, as shown in Fig. 6(a). In order to reduce the energy consumption, microwave discharge was operated in a pulse mode, as shown in Fig. 6(b). The duty cycle and the pulse period were varied within 0.2–1.0 and 0.01–1.0 ms region, respectively. Figures 7 and 8 show the dependence of the conversion of NO and the formation ratios of products in an NO/Ar mixture on the duty cycle and the

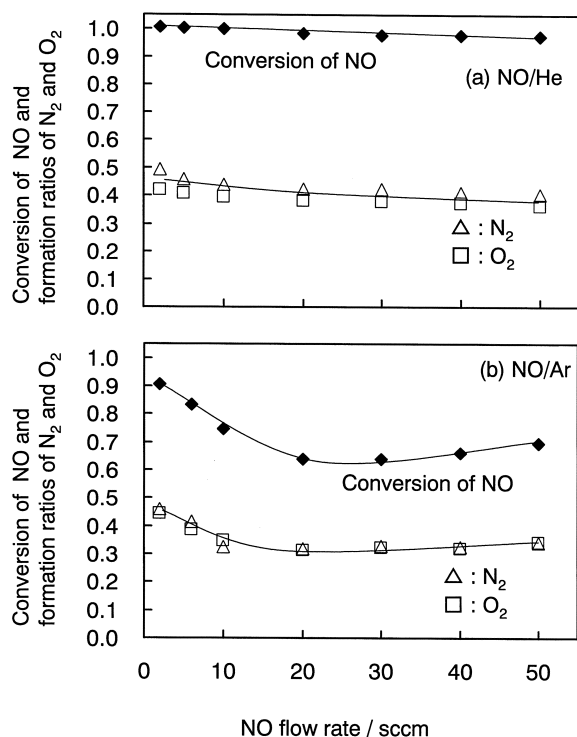
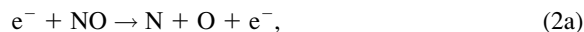


Fig. 4. Dependence of conversion of NO and formation ratios of  $N_2$  and  $O_2$  on the NO flow rate in NO/He mixtures at a total pressure of 100 Torr and in NO/Ar mixtures at a total pressure of 760 Torr. The initial concentration of NO was 2000–47600 ppm and the microwave power was 200 W.

pulse period, respectively, at a microwave power of 200 W. The conversion of NO increases from 31 to 63% with increasing duty cycle from 0.2 to 1.0. The effective microwave power is 50 W at a duty cycle of 0.25. The conversion of NO at an effective microwave power of 50 W is about 32%, which is larger than that at 50 W in a continuous mode (about 20% in Fig. 5(b)). Thus, the pulse mode is more effective for the reduction of energy consumption, though the conversion of NO is low in such a low duty cycle. In Fig. 8, the conversion of NO was measured as a function of the pulse period at a constant duty cycle of 0.5. The conversion of NO slightly increases from 34 to 46% with increasing the pulse period from 0.01 to 1 ms. Thus, a long pulse period is better for the effective decomposition of NO in a pulsed microwave discharge of the NO/Ar mixture at 760 Torr.

**Decomposition Mechanism of NO/He and NO/Ar Mixtures by Microwave Discharge.** In the microwave discharge of NO/He mixtures, possible active species are electrons, metastable  $He(2^3S)$  atoms, and  $He^+$ . Therefore, in addition to direct electron-impact dissociation and ionization processes (2a)–(2b) by accelerated electrons,<sup>16</sup> Penning ionization (3a) and (3b) by  $He(2^3S)$ , and charge-transfer reactions (4b) and (4c) by  $He^+$  can take part in the decomposition and ionization of NO:



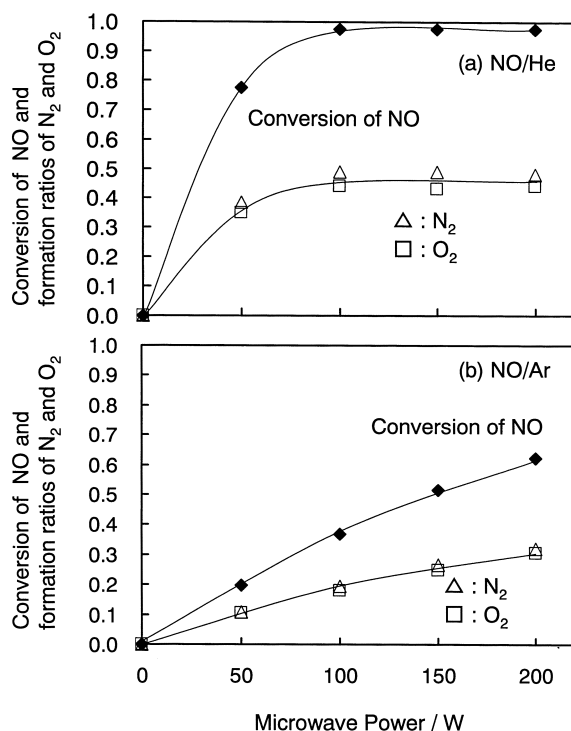


Fig. 5. Dependence of conversion of NO and formation ratios of  $N_2$  and  $O_2$  on the microwave power in an NO/He mixture at a total pressure of 100 Torr and in an NO/Ar mixture at a total pressure of 760 Torr. The NO flow rate was 25 sccm corresponding to its initial concentration of 24400 ppm.

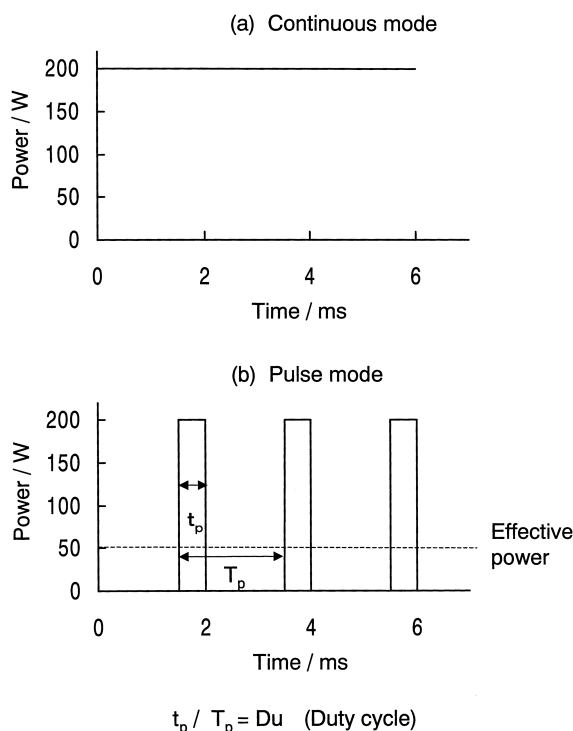


Fig. 6. Continuous and pulsed microwave discharges

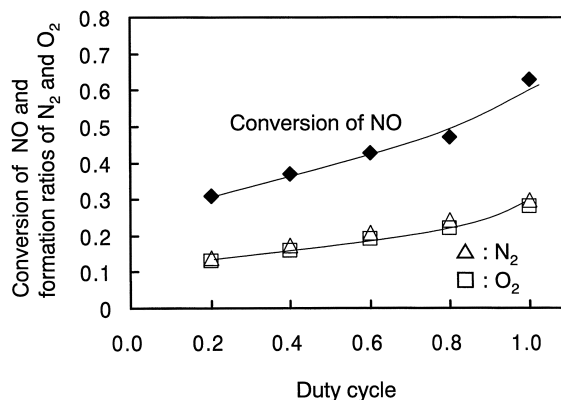


Fig. 7. Dependence of conversion of NO and formation ratios of  $N_2$  and  $O_2$  on the duty cycle in NO/Ar mixtures at a total pressure of 760 Torr and a microwave power of 200 W. The NO flow rate was 25 sccm corresponding to its initial concentration of 24400 ppm.

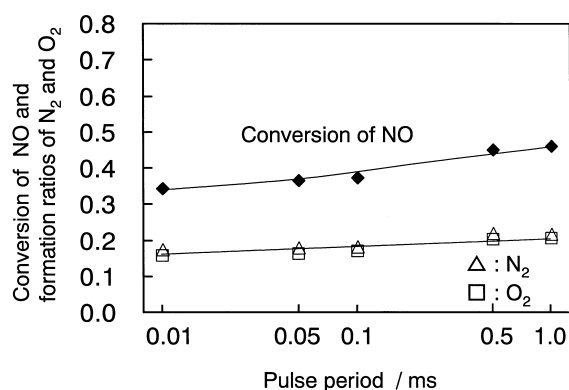
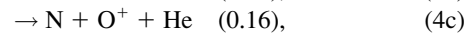
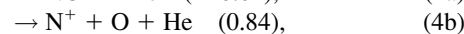
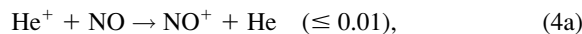


Fig. 8. Dependence of conversion of NO and formation ratios of  $N_2$  and  $O_2$  on the pulse period in NO/Ar mixtures at a duty cycle of 0.5, a total pressure of 760 Torr, and a microwave power of 200 W. The NO flow rate was 25 sccm corresponding to its initial concentration of 24400 ppm.

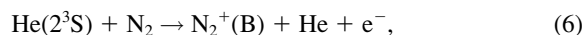
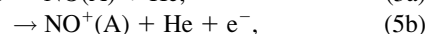
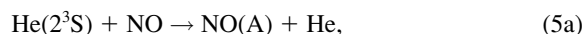


$$k_3(\text{total}) = 2.0 \times 10^{-10} \text{ cm}^3 \text{ molecule}^{-1} \text{ s}^{-1},^{17}$$



$$k_4(\text{total}) = 1.6 \times 10^{-9} \text{ cm}^3 \text{ molecule}^{-1} \text{ s}^{-1}.^{18}$$

If  $\text{He}(2^3\text{S})$  and  $\text{He}^+$  participate in the formation of neutral products, the  $\text{NO}(A^2\Sigma^+ - X^2\Pi_r)$ ,  $\text{NO}^+(A^1\Pi - X^1\Sigma^+)$ ,  $\text{N}_2^+(\text{B}^2\Sigma_u^+ - X^2\Sigma_g^+)$ , and  $\text{N}_2^+(\text{C}^2\Sigma_u^+ - X^2\Sigma_g^+)$  emissions, resulting from the following excitation transfer, Penning ionization, and charge-transfer reactions of NO and  $\text{N}_2$ , must be observed in the discharge region on the basis of previous optical spectroscopic studies:<sup>19–24</sup>



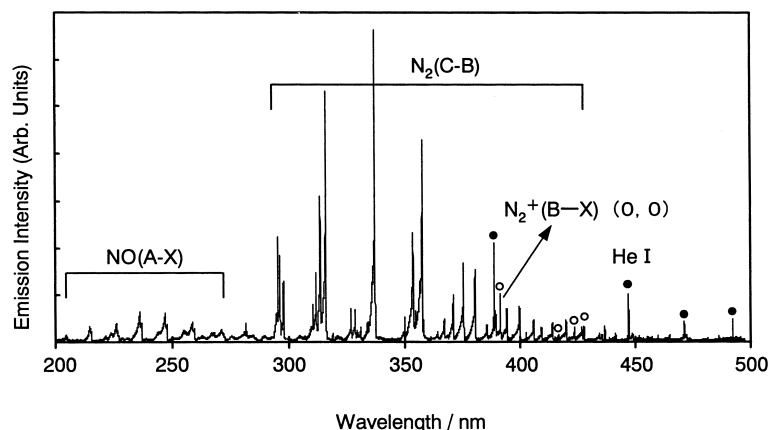
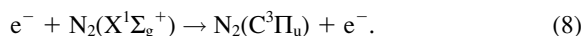


Fig. 9. Emission spectrum of NO/He discharge at an NO flow rate of 100 sccm, a total pressure of 0.5 Torr, and a microwave power of 200 W. The initial concentration of NO was 90900 ppm. Lines marked by ● and ○ indicate He\* atomic lines and the  $N_2^+(B-X)$  transition, respectively.



It is possible to observe the NO(A-X),  $N_2^+(B-X)$ , and  $N_2^+(C-X)$  emissions in the 190–600 nm region. However, the  $\text{NO}^+(\text{A-X})$  emission could not be detected in this study because of its appearance in the vacuum UV region.<sup>19,22</sup> In order to obtain information on the major decomposition mechanism, we measured emission spectra of the microwave discharge of an NO/He mixture in the UV and visible region. Figure 9 shows a typical emission spectrum in the 200–500 nm region, where a strong  $N_2(\text{C}^3\Pi_u-\text{X}^3\Pi_g)$  emission, weak  $\text{NO}^+(\text{A}^2\Sigma^+-\text{X}^2\Pi_r)$  and  $N_2^+(\text{B}^2\Sigma_u^+-\text{X}^2\Sigma_g^+)$  emissions, and He\* atomic lines are identified. The observed spectrum was essentially independent of the NO flow rate. The lack of  $N_2^+(\text{C-X})$  emissions led us to conclude that  $\text{He}^+$  is not a dominant active species under the operating conditions. A stable microwave discharge could be maintained using pure NO at a high flow rate of 100 sccm. The emission spectrum of the microwave discharge of pure NO gas, where He( $2^3\text{S}$ ) was absent, was very similar to that observed from the discharge of the NO/He mixture. In the previous study,<sup>2</sup> we measured optical emission spectra resulting from the reactions of He( $2^3\text{S}$ ) with discharge products of NO/He mixture using an additional microwave-discharge source of He( $2^3\text{S}$ ). Although a strong  $N_2^+(B-X)$  emission due to Penning ionization (6) was observed, no  $N_2(\text{C-B})$  emission was found. In this study, such a strong  $N_2^+(B-X)$  emission could not be detected, though a strong  $N_2(\text{C-B})$  emission was observed. On the basis of the above findings, it is reasonable to assume that He( $2^3\text{S}$ ) is not a major active species under the operating conditions. Thus, electrons accelerated by an electric field in the microwave discharge, will be a major active species for the decomposition of NO diluted in He.

It is known that neutral  $N_2(\text{C}^3\Sigma_u-B^3\Pi_g)$  emission results from electron-impact excitation of  $N_2$ .<sup>25,26</sup>

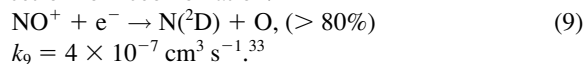


The dependence of the emission cross section of the  $N_2(\text{C}^3\Pi_u-B^3\Pi_g)$  transition on the electron energy, which is called the excitation function of  $N_2(\text{C})$ , has been measured. The excitation function of  $N_2(\text{C})$  in the optically forbidden singlet  $\rightarrow$  triplet

process (8) has a sharp peak at about 14 eV, which decreases rapidly with increasing electron energy.<sup>25,26</sup> On the other hand, the  $N_2^+(B-X)$  emission appears at high electron energies above its threshold energy of 18.8 eV for the ground state  $N_2(\text{X}^1\Sigma_g^+)$  molecule.<sup>27</sup> However, the minimum energy required for the formation of  $N_2^+(\text{B})$  from  $N_2^+(\text{X}^2\Sigma_g^+)$  is only 3.2 eV. The relative contribution of  $N_2(\text{X})$  and  $N_2^+(\text{X})$  for the formation of  $N_2^+(\text{B})$  was examined by the extent of vibrational excitation of the  $N_2^+(B-X)$  emission. It is known that vibrational relaxation of  $N_2(\text{X}; v'' > 0)$  by collisions with  $N_2$  is very slow in a helium flow,<sup>23,24,28–30</sup> while that of  $N_2^+(\text{X}; v'' > 0)$  is very fast.<sup>31,32</sup> Besides the  $N_2^+(B-X)$  emission from  $v' = 0$ , that from  $v' = 1–3$  is identified in this study, as shown in Fig. 9. It is therefore highly likely that the  $N_2^+(B-X)$  emission in Fig. 9 arises from electron-impact ionization of  $N_2(\text{X})$ . The observation of the strong  $N_2(\text{C-B})$  emission and the weak  $N_2^+(B-X)$  emission indicates that the energy distribution of electrons at 14 eV is larger than that at about 19 eV.

In addition to the above electron-impact dissociative excitation processes, the subsequent secondary two-body and three-body reactions will occur, finally leading to the formation of  $N_2$  and  $\text{O}_2$  products. Among them, major secondary reactions at low pressures will be as follows:

Electron-ion recombination:



Two-body reaction between  $\text{N}(\text{D})$  and NO:



$$k_{10a} = (3.3 \pm 1.5) \times 10^{-11} \text{ cm}^3 \text{ molecule}^{-1} \text{ s}^{-1},^{34,35}$$

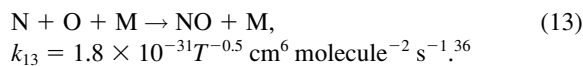
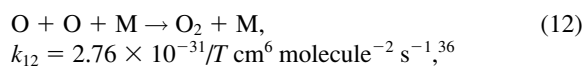
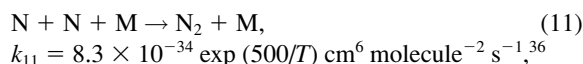


$$k_{10b} = (6.3 \pm 2.0) \times 10^{-11} \text{ cm}^3 \text{ molecule}^{-1} \text{ s}^{-1}.^{34,35}$$

In the electron-ion recombination process (9),  $\text{NO}^+$  ions dominantly result from process (2b), while slow electrons are generated via processes (2b)–(2d). Fast two-body reactions between  $\text{N}(\text{D})$  and NO, (10a) and (10b), will be major production processes of  $N_2$  in our conditions.

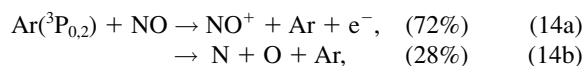
At high pressures, the following three-body recombination processes may also be responsible for the formation of  $N_2$ ,  $\text{O}_2$ ,

and NO:

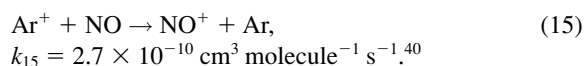


Here, M represents third-body NO, N<sub>2</sub>, O<sub>2</sub>, and He. Two-body rate constants of the three recombination reactions (11)–(13) are calculated to be  $1.4 \times 10^{-16}$ ,  $3.0 \times 10^{-17}$ , and  $3.4 \times 10^{-16}$  cm<sup>3</sup> molecule<sup>-1</sup> s<sup>-1</sup> at a M pressure of 1 Torr and 300 K and  $1.1 \times 10^{-13}$ ,  $2.3 \times 10^{-14}$ , and  $2.6 \times 10^{-13}$  cm<sup>3</sup> molecule<sup>-1</sup> s<sup>-1</sup> at a M pressure of 760 Torr and 300 K, respectively, from the relation  $k_{\text{rel}}[\text{M}]$  for  $x = 11$ –13. Since the calculated constants of (11) at 1–760 Torr are much smaller than those of processes (10a) and (10b), three-body reaction (11) will be less significant than two-body reactions (10a) and (10b). On the other hand, the two-body reaction of O(<sup>3</sup>P) with NO is negligibly slow and the two-body reaction of O(<sup>1</sup>S) with NO gives O(<sup>3</sup>P) + NO with a rate constant of  $4.0 \times 10^{-11}$  cm<sup>3</sup> molecule<sup>-1</sup> s<sup>-1</sup> at 300 K.<sup>34–38</sup> Therefore, it is expected that O<sub>2</sub> is dominantly produced via three-body reaction (12) in our conditions. The formation ratio of O<sub>2</sub> was nearly identical to that of N<sub>2</sub> at total pressures above 50 Torr, as shown in Figs. 3(a) and 3(b). This result was consistent with the prediction from Eq. 1. The formation ratio of O<sub>2</sub> became smaller than that of N<sub>2</sub> with decreasing the total pressure from about 30 Torr, though it is not shown in Figs. 3(a) and 3(b). This finding can be explained by the fact that the total pressure was too low to completely convert O atom to O<sub>2</sub> via three-body reaction (12) below about 30 Torr. The above results support our prediction that three-body reaction (12) is dominantly responsible for the formation of O<sub>2</sub> under our conditions.

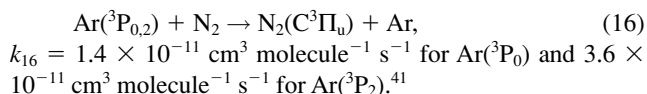
In NO/Ar mixtures, metastable Ar(<sup>3</sup>P<sub>0,2</sub>) atoms and Ar<sup>+</sup>(<sup>2</sup>P<sub>1/2,3/2</sub>) ions can be formed as possible active species by electron-impact excitation and ionization of Ar, instead of He(<sup>2</sup>S) and He<sup>+</sup> in NO/He mixtures. These species can induce the following reactions:



$$k_{14}(\text{total}) = 2.2 \times 10^{-10} \text{ cm}^3 \text{ molecule}^{-1} \text{ s}^{-1}.^{39}$$



If Ar(<sup>3</sup>P<sub>0,2</sub>) exists in the reaction region as responsible species for the formation of neutral products, the N<sub>2</sub>(C<sup>3</sup>Π<sub>u</sub>-B<sup>3</sup>Π<sub>g</sub>) emission must be observed:



The spectrum observed from NO/Ar mixtures was similar to

that in NO/He discharge, where a strong N<sub>2</sub>(C-B) emission, weak NO(A-X) emission and N<sub>2</sub><sup>+</sup>(B-X) emission from  $v' = 0$  and 1, and Ar<sup>+</sup> atomic lines were observed. Since the N<sub>2</sub><sup>+</sup>(B-X) emission from  $v' = 1$  was observed, N<sub>2</sub><sup>+</sup>(B) must be dominantly formed by direct electron-impact ionization of N<sub>2</sub>(X). At the present time, it is difficult to distinguish whether the N<sub>2</sub>(C-B) emission arises from Ar(<sup>3</sup>P<sub>0,2</sub>)/N<sub>2</sub> reaction (16) or electron-impact excitation of N<sub>2</sub> (8). Therefore, not only accelerated electrons but also Ar(<sup>3</sup>P<sub>0</sub>) and Ar(<sup>3</sup>P<sub>2</sub>) with available energies of 11.75 and 11.55 eV, respectively, may contribute to the decomposition of NO via direct decomposition process (14b) and via Penning ionization (14a) followed by recombination process (9). Since the ionization energy of Ar(15.76 eV) is much lower than that of He(24.59 eV), Ar<sup>+</sup> can be formed in Ar discharge more easily than He<sup>+</sup> in He discharge. Therefore, Ar<sup>+</sup> may also participate in the decomposition of NO through direct decomposition processes (15) followed by recombination process (9), though a further experimental study is required to determine its relative contribution.

The upper limit of the total pressure in NO/He mixtures, which is necessary to maintain stable discharge, was much lower than that in NO/Ar mixtures at an NO flow rate of 25 sccm and a microwave power of 200 W. High-energy electrons are required to maintain stable He discharge because of a high ionization energy of He (24.59 eV). Therefore, it becomes difficult to maintain stable discharge at high NO/He pressures due to decrease in electron temperature. On the other hand, such high-energy electrons are unnecessary for the operation of Ar discharge, and discharge can be maintained by electrons with energies higher than 15.76 eV. Thus, the operation of discharge of NO/Ar mixtures is possible at high NO/Ar pressures, even though the mean free path of electrons becomes short.

Although the upper limit of the total pressure for the NO/He mixture was much lower than that for the NO/Ar mixture, an advantage of NO/He mixtures was the higher conversion of NO below the total pressure of 350 Torr. Since the electron temperature of the NO/He mixture is higher than that of the NO/Ar mixture, high-energy electrons decompose NO more efficiently within the discharge region. Thus, the conversion of NO in the NO/He mixture will be larger than that in the NO/Ar one. The conversion of NO using a pulsed microwave discharge was larger than that using a continuous one. The electric field in a pulse mode is larger than that in a continuous mode by a factor of  $1/(\text{Du})^{1/2}$ , where Du is the duty cycle of pulse (see Fig. 6).<sup>42</sup> Thus, a higher conversion of NO in the pulse mode can be attributed to the fact that a higher electric field in the discharge is more effective than the pulse period for the decomposition of NO.

Although extensive studies have recently been carried out to remove NO using a microwave discharge,<sup>2–9</sup> microwave absorbers and catalysts were simultaneously used to stabilize and improve NO conversion in all of the previous studies except for our previous work<sup>2</sup> and a study of Wójtowicz et al.<sup>3</sup> Wójtowicz et al. have studied the decomposition of NO by a microwave discharge of NO/N<sub>2</sub> mixtures. They reported that 98% of NO is decomposed at the total pressure range of 10–234 Torr, an NO concentration of 6000 ppm, and a microwave power of 250 W, though the discharge products were not analyzed. In

this work, we studied the decomposition of NO by a microwave discharge of NO/He and NO/Ar mixtures at the NO concentration of 24400 ppm and 2000–47600 ppm, respectively. The conversion of NO in the NO/He mixture at an NO concentration of 24400 ppm was 95–98% over the total pressure range of 50–250 Torr, while that in NO/Ar mixtures at an NO concentration of 6000 ppm was 83% over the same total pressure range. On the basis of the above findings, it is concluded that the decomposition efficiency of NO in NO/N<sub>2</sub> mixtures at the total pressure range of 10–234 Torr is higher than that in NO/Ar mixtures and is comparable with that in NO/He mixtures. Unfortunately, it was difficult to compare the energy required for the decomposition of NO between the present results and previous data of Wójtowicz et al.,<sup>3</sup> because they did not report the NO/N<sub>2</sub> flow rate in each experiment.

### Conclusion

In conclusion, NO was decomposed by a microwave discharge of NO/He or NO/Ar mixtures without using catalysts and microwave absorbents such as Co<sub>3</sub>O<sub>4</sub> and SiC. Optical emission spectroscopic data of NO/He or NO/Ar discharges indicated that major active species for the decomposition of NO in NO/He mixtures were electrons accelerated by an electric field, and those in NO/Ar mixtures were accelerated electrons and/or metastable Ar(<sup>3</sup>P<sub>0,2</sub>) atoms. Under our experimental conditions, stable discharge could be maintained below 350 Torr in NO/He mixtures and below 760 Torr in NO/Ar mixtures. The conversion of NO in the NO/He mixture below 350 Torr ( $\geq 93\%$ ) was higher than that in the NO/Ar one ( $\geq 67\%$ ). It was explained as due to the higher electron temperature in NO/He mixtures, which can effectively decompose NO into N<sub>2</sub> and O<sub>2</sub>. A high decomposition efficiency of 90% was obtained in the NO/Ar mixture at an NO concentration of 2000 ppm and a total pressure 760 Torr. We are planning to extend this study to the decomposition of NO under atmospheric pressure in the presence of N<sub>2</sub>, O<sub>2</sub>, and H<sub>2</sub>O for the practical application of the microwave discharge to NO<sub>x</sub> removal.

The authors acknowledge financial support from a Grant-in-Aid for Scientific Research No. 13558056 from the Ministry of Education, Science, Sports and Culture, and from Kyushu University Interdisciplinary Programs in Education and Projects in Research Development (2001).

### References

- 1 J. S. Chang, *Oyo Butsuri*, **69**, 268 (2000), and references therein.
- 2 M. Tsuji, A. Tanaka, T. Hamagami, K. Nakano, and Y. Nishimura, *Jpn. J. Appl. Phys.*, **39**, L933 (2000).
- 3 M. A. Wójtowicz, F. P. Miknis, R. W. Grimes, W. W. Smith, and M. A. Serio, *J. Hazardous Materials*, **74**, 81 (2000).
- 4 H. S. Roh, Y. K. Park, and S. E. Park, *Chem. Lett.*, **2000**, 578.
- 5 J. Tang, T. Zhang, D. Liang, X. Sun, and L. Lin, *Chem. Lett.*, **2000**, 916.
- 6 J. Tang, T. Zhang, D. Liang, C. C. Xu, X. Sun, and L. Lin, *Chem. Commun.*, **2000**, 1861.
- 7 J. Tang, T. Zhang, D. Liang, X. Sun, and L. Lin, *Chem. Lett.*, **2001**, 140.
- 8 J. Tang, T. Zhang, L. Ma, L. Li, J. Zhao, M. Zheng, and L. Lin, *Catal. Lett.*, **73**, 193 (2001).
- 9 M. Baeva, M. Gier, A. Pott, L. Uhlenbusch, J. Hoschele, and J. Steinwandel, *Plasma Chem. Plasma Process.*, **21**, 225 (2001).
- 10 Y. S. Mok and I. S. Nam, *J. Chem. Eng. Jpn.*, **31**, 391 (1998).
- 11 A. Harano, Y. Imaizumi, and M. Sadakata, *J. Chem. Eng. Jpn.*, **31**, 694 (1998).
- 12 G. Sthiamoorthy, S. Kalyana, W. C. Finney, and B. R. Locke, *Ind. Eng. Chem. Res.*, **38**, 1844 (1999).
- 13 K. Takaki, M. A. Jani, and T. Fujiwara, *IEEE Trans. Plasma Sci.*, **27**, 1137 (1999).
- 14 M. Tsuji, T. Tanoue, K. Nakano, A. Tanaka, and Y. Nishimura, *Jpn. J. Appl. Phys.*, **39**, L1330 (2000).
- 15 M. Tsuji, T. Tanoue, J. Kumagae, and K. Nakano, *Jpn. J. Appl. Phys.*, **40**, 7091 (2001).
- 16 B. G. Lindsay, M. A. Mangan, H. C. Straub, and R. F. Stebbings, *J. Chem. Phys.*, **112**, 9404 (2000).
- 17 R. S. F. Chang, D. W. Setser, and G. W. Taylor, *Chem. Phys.*, **35**, 201 (1978).
- 18 V. G. Anicich, J. B. Laudenslager, W. T. Hunstres Jr., and J. H. Futrell, *J. Chem. Phys.*, **67**, 4340 (1977).
- 19 J. A. Coxon, M. A. A. Clyne, and D. W. Setser, *Chem. Phys.*, **7**, 255 (1975).
- 20 M. Endoh, M. Tsuji, and Y. Nishimura, *J. Chem. Phys.*, **79**, 5368 (1983).
- 21 H. Sekiya, M. Tsuji, and Y. Nishimura, *J. Chem. Phys.*, **87**, 325 (1987).
- 22 M. Tsuji, Y. Nishimura, H. Ishimi, M. Hisano, and H. Oota, *J. Chem. Phys.*, **110**, 9064 (1999).
- 23 M. Tsuji, *Houshasen Kagaku*, **71**, 33 (2001).
- 24 M. Tsuji, T. Tsuji, T. Hamagami, and K. Nakano, *J. Chem. Phys.*, **115**, 6811 (2001).
- 25 W. L. Borst and E. C. Zipf, *Phys. Rev. A*, **1**, 834 (1970).
- 26 T. G. Finn, J. F. M. Aarts, and J. P. Doering, *J. Chem. Phys.*, **56**, 5632 (1972).
- 27 M. Imami and W. L. Borst, *J. Chem. Phys.*, **61**, 1115 (1974).
- 28 S. J. Young, *J. Chem. Phys.*, **58**, 1603 (1973).
- 29 J. Jolly, M. Touzeau, and A. Richard, *J. Phys. B*, **14**, 473 (1981).
- 30 L. G. Piper and W. J. Marinelli, *J. Chem. Phys.*, **89**, 2918 (1988).
- 31 H. Sekiya, T. Hirayama, M. Endoh, M. Tsuji, and Y. Nishimura, *Chem. Phys.*, **101**, 291 (1986).
- 32 K. Sohlberg, *Chem. Phys.*, **246**, 307 (1999).
- 33 L. Vejby-Christensen, D. Kella, H. B. Pedersen, and L. H. Andersen, *Phys. Rev. A*, **57**, 3627 (1998).
- 34 D. L. Baulch, R. A. Cox, P. J. Crutzen, R. F. Hampson, Jr., J. A. Kerr, J. Troe, and R. T. Watson, *J. Phys. Chem. Ref. Data*, **11**, 327 (1982).
- 35 D. L. Baulch, R. A. Cox, P. J. Crutzen, R. F. Hampson, Jr., J. A. Kerr, J. Troe, and R. T. Watson, *J. Phys. Chem. Ref. Data*, **13**, 1259 (1984).
- 36 M. Mätzing, *Adv. Chem. Phys.*, **80**, 315 (1991), and references therein.
- 37 K. Schofield, *J. Phys. Chem. Ref. Data*, **8**, 723 (1979).
- 38 "Kagaku Binran," 4th ed., ed by Chem. Soc. Jpn., Maruzen, Tokyo (1993).
- 39 M. T. Jones, T. D. Dreiling, D. W. Setser, and R. N. McDonald, *J. Phys. Chem.*, **89**, 4501 (1985).

- 40 R. J. Shul, B. L. Upschulte, R. Passarella, R. G. Keesee,  
and A. W. Castleman, Jr., *J. Phys. Chem.*, **91**, 2556 (1987).  
41 N. Sadeghi, M. Cheaib, and D. W. Setser, *J. Chem. Phys.*,

**90**, 219 (1989).

- 42 “The Compilation of Microwave Heating Technologies,”  
ed by T. Koshijima, NTS (1994), p. 733.